$Ge_2Sb_2Se_5$ Glass as High-Capacity Promising Lithium-ion Battery Anode

Jassiel R. Rodriguez,[1,*] Zhimin Qi,[2] Haiyan Wang,[2] Mikhail Y. Shalaginov,[3] Claudia Goncalves,[4] Myungkoo Kang,[4] Kathleen A. Richardson,[4] J. Guerrero-Sanchez,[5] Ma Guadalupe Moreno-Armenta,[5] Vilas G. Pol[1]

[1]*Davidson School of Chemical Engineering, Purdue University, West Lafayette, IN 47907, USA.*

[2]*School of Materials Engineering, Purdue University, West Lafayette, IN 47907, USA.*

[3]*Department of Materials Science and Engineering, Massachusetts Institute of Technology, Cambridge, MA 02139, USA.*

[4]*College of Optics and Photonics, Department of Materials Science and Engineering, University of Central Florida, Orlando, FL 32816, USA.*

[5]*Centro de Nanociencias y Nanotecnología, Universidad Nacional Autónoma de México, Ensenada, BC 22860, Mex.*

Corresponding author: rodri571@purdue.edu

Table S1. Summarized nearest neighbor distances between Ge, Sb and Se atoms in a glassy GSS arrangement.

Atom		Coordination	Nearest neighbor distances (Å)
Ge	Sb	3	3.66 - 3.99
Ge	Ge	-	3.55 - 4.0
Ge	Se	3	2.22 - 2.9
Se	Sb	3, 4	2.58 - 2.99
Se	Se	-	3.81 - 4.0
Sb	Sb	-	3.73 - 4.2

Figure S1.

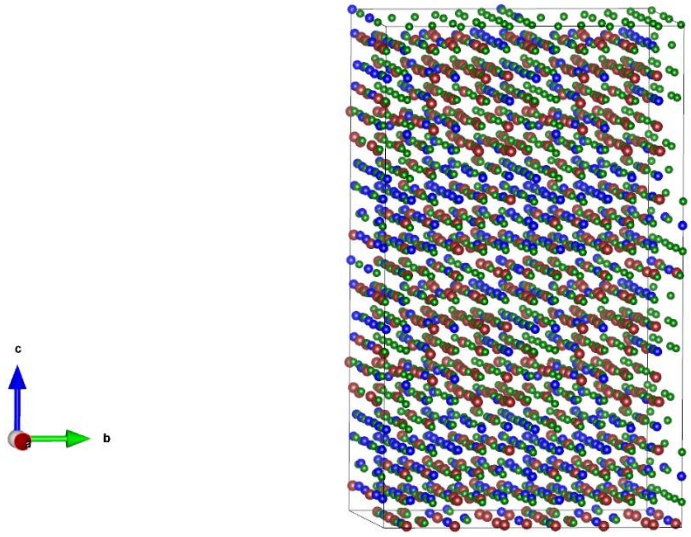

Figure S1. 2x2x2 supercell of the glassy GSSe simulated atomic arrangement, Se (green), Ge (blue) and Sb (red)

Figure S2.

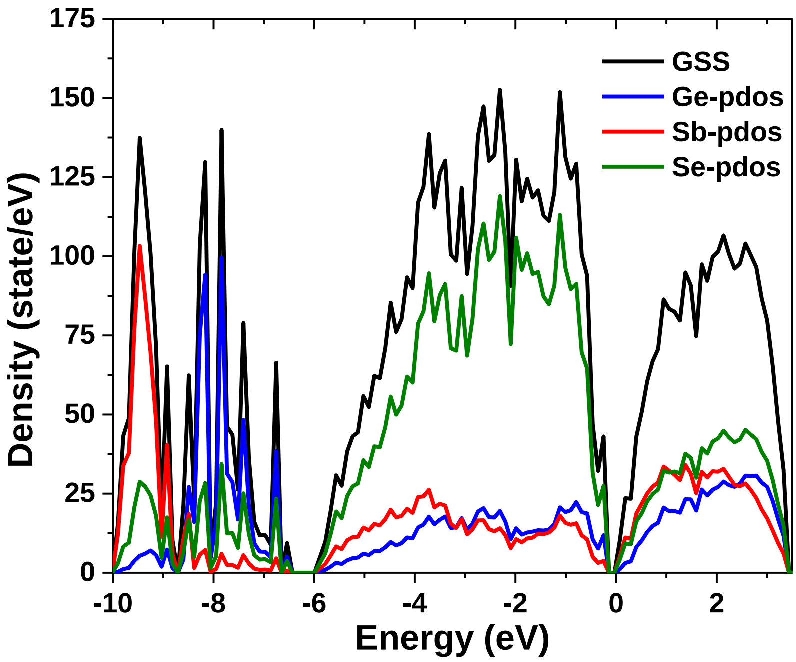

Figure S2. Calculated and projected density of states of glassy GSSe anode.

Figure S3.

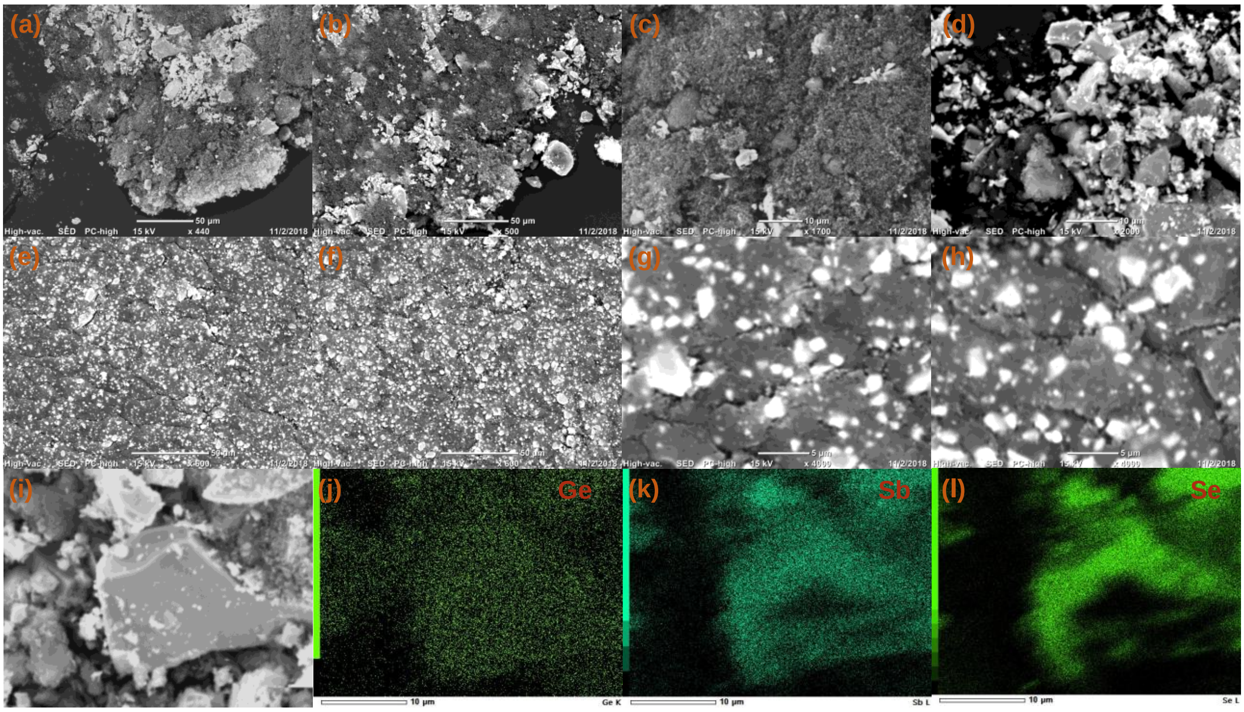

Figure S3. Topographic information of (a–d) raw GSSe particles, (e–h) GSSe-carbon composite, and (i–l) elemental mapping of raw glassy GSSe particle.

Figure S4.

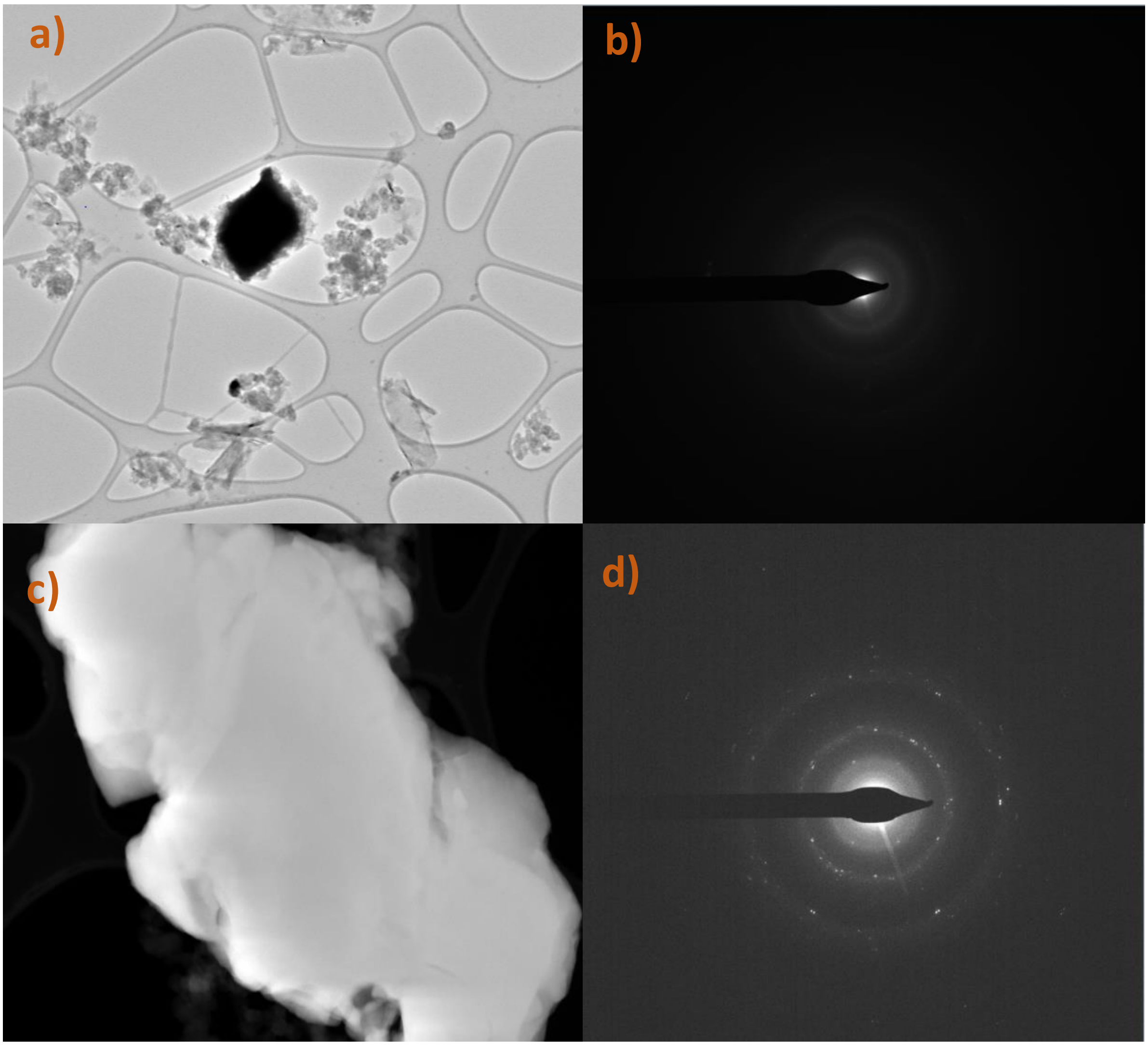

Figure S4. Microstructural and crystalline information of glassy GSSe particles: (a,c) low resolution TEM micrographs and (b,d) electron diffraction pattern of individual GSSe particles.

Figure S5.

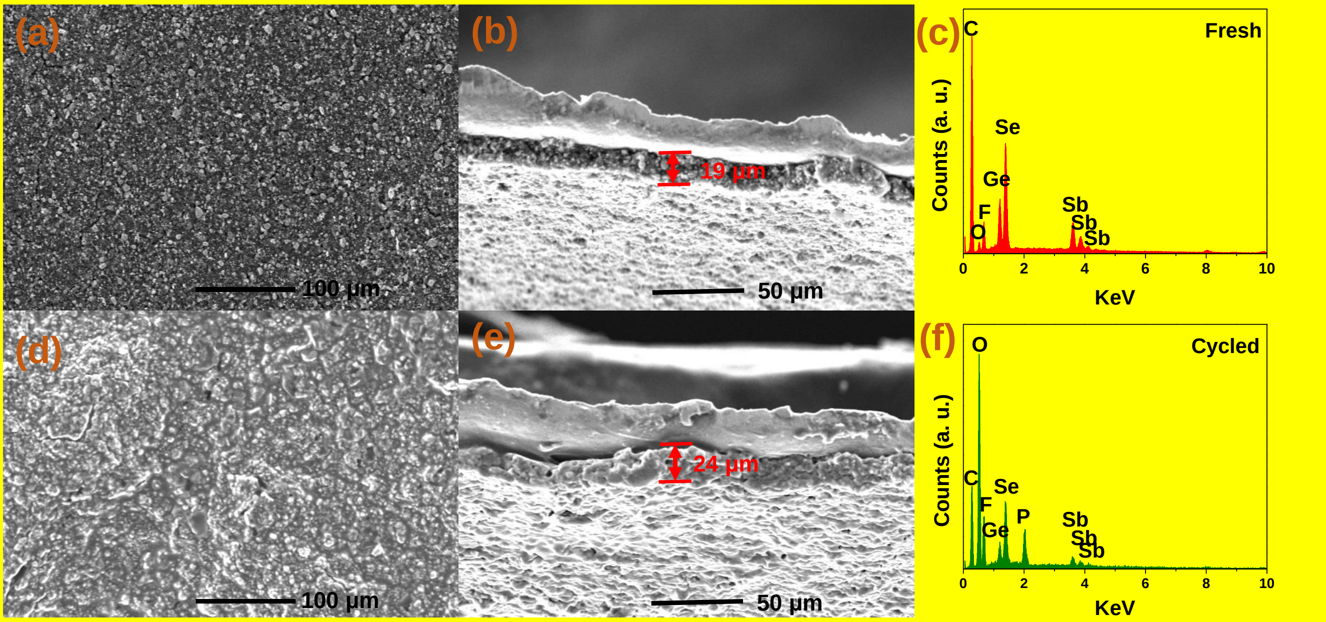

Figure S5. Frontal and cross-section images from (a, b) fresh and (d, e) cycled GSSe electrodes. Elemental analysis of (c) fresh and (f) cycled GSSe electrodes.

Figure S6.

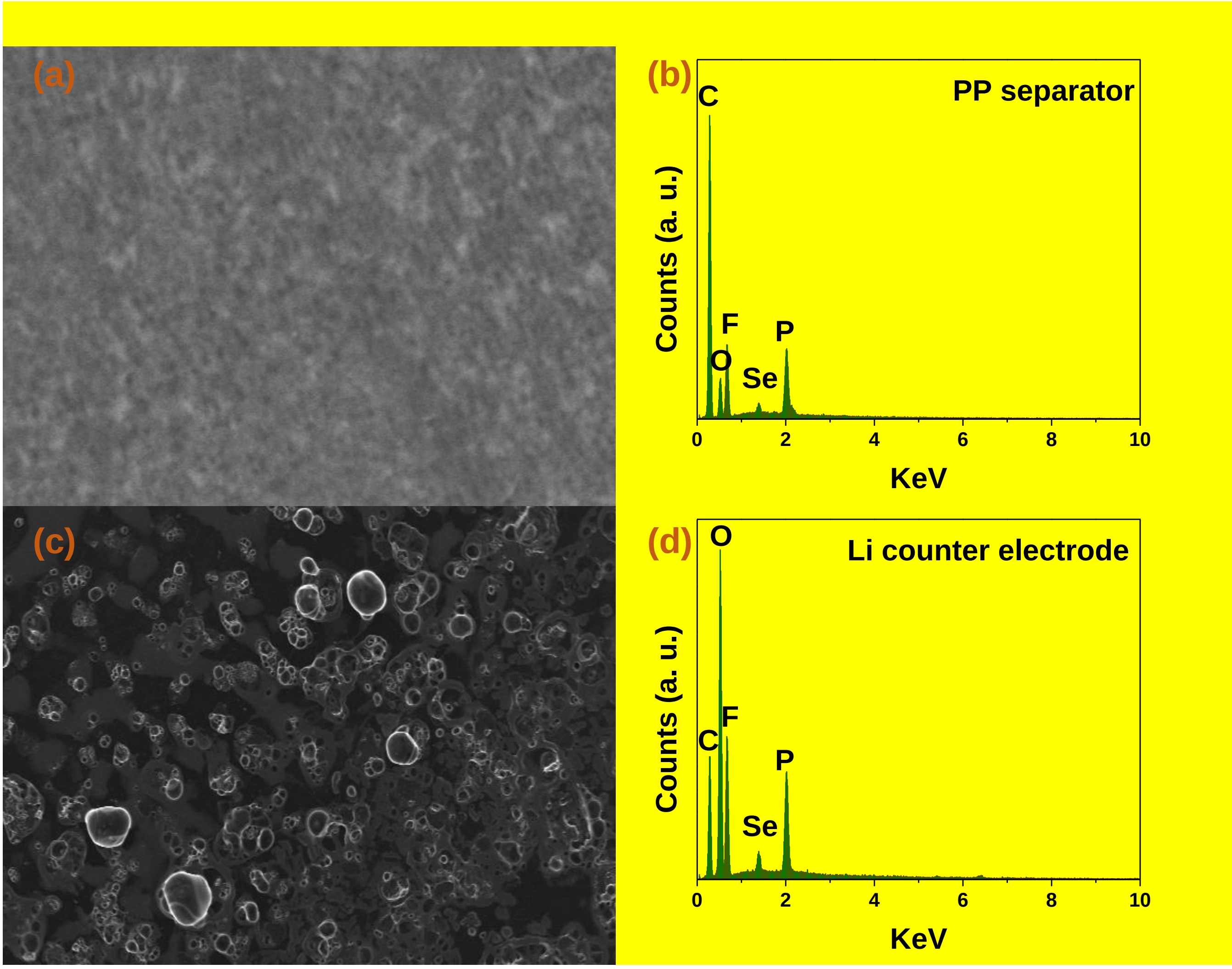

Figure S6. SEM images from the cycled (a) PP separator and (c) Li disk with their corresponding EDS analysis, reveling the presence of Se on both parts.

Figure S7

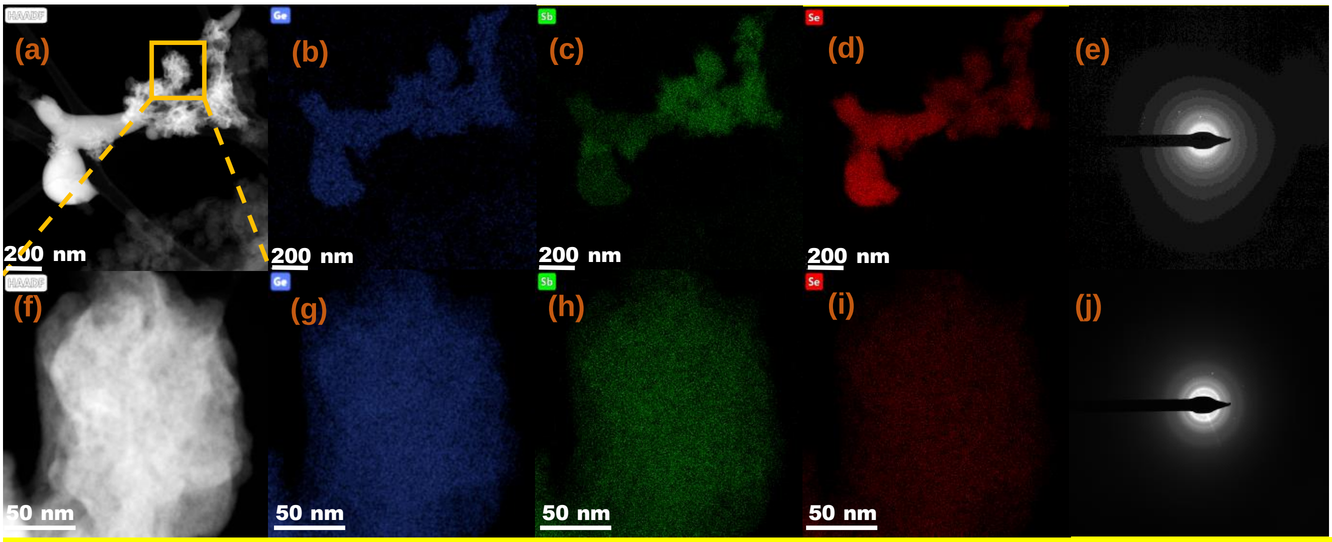

Figure S7. Microstructural, crystalline and chemical information of the GSSe electrode after 100 cycles: (a) low- and (f) high-resolution TEM micrographs; EDS analysis of the cycled GSSe electrode, Ge (blue), Sb (green) and Se (red); selected-area electron diffraction pattern of (e) Se-rich and (j) Se-poor regions.

Figure S8.

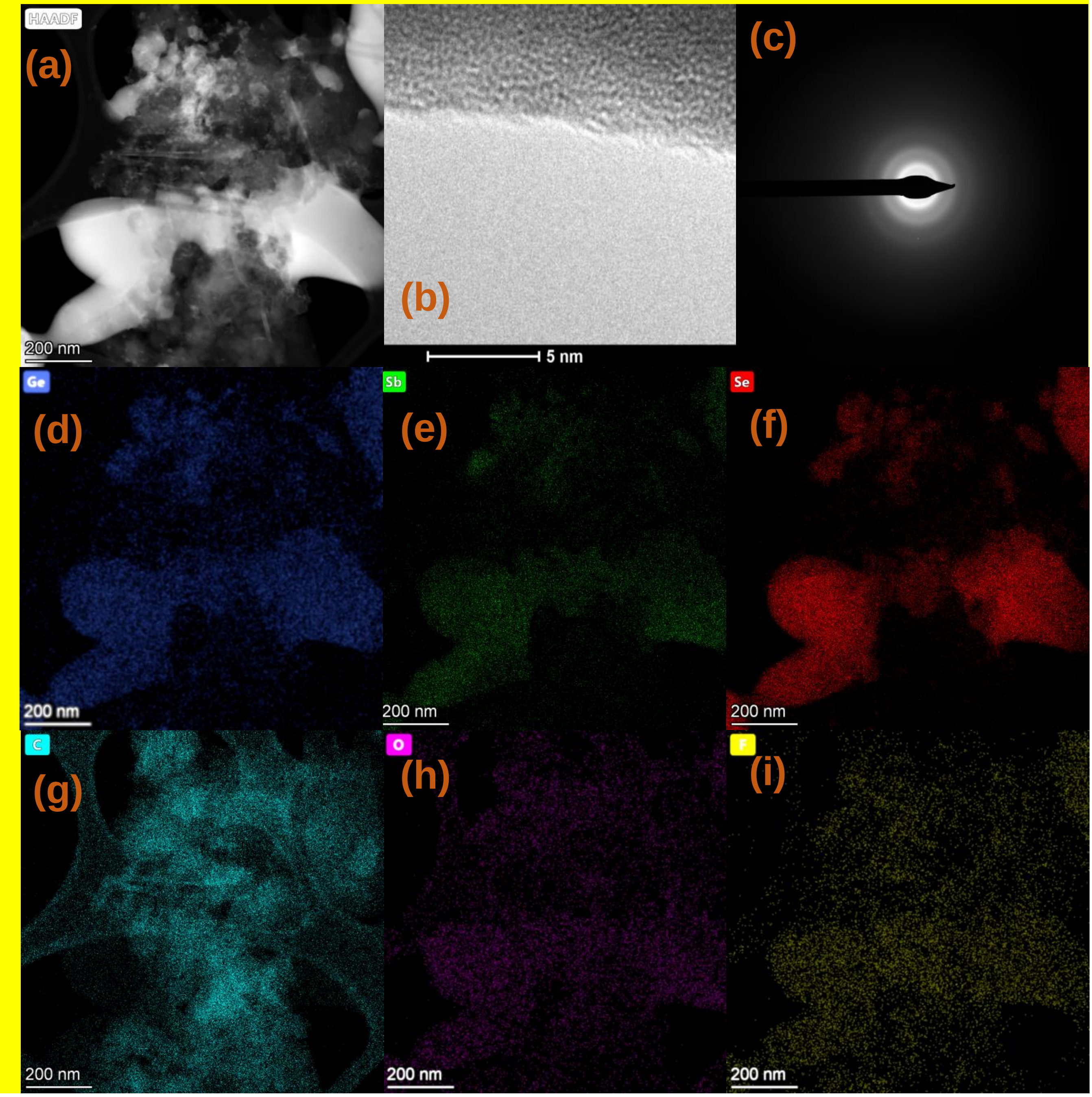

Figure S8. Microstructural, crystalline and chemical information of the GSSe electrode after 1st cycle: (a) low- and (b) high-resolution TEM micrographs; (c) selected-area electron diffraction pattern; (d)-(i) EDS analysis of the cycled GSSe electrode, Ge (blue), Sb (green), Se (red), carbon (cyan), oxygen (indigo) and fluorine (yellow).

Figure S9.

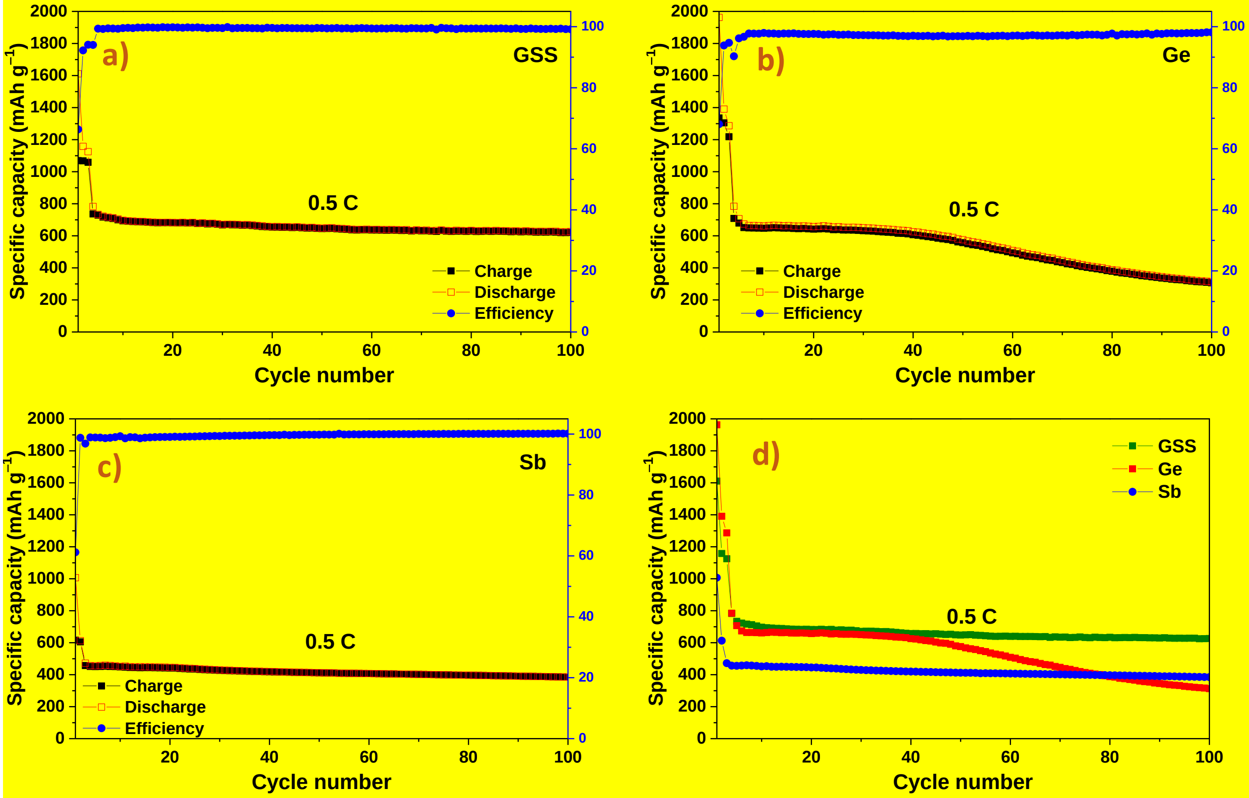

Figure S9. Cycle performance of (a) GSSe powder, (b) Ge nanoparticles and (c) Sb nanoparticles. (d) Comparison of discharge capacity delivered by GSSe, Ge and Sb during 100 cycles between 0.01 and 3.0 V vs Li/Li^{+}.

Figure S10.

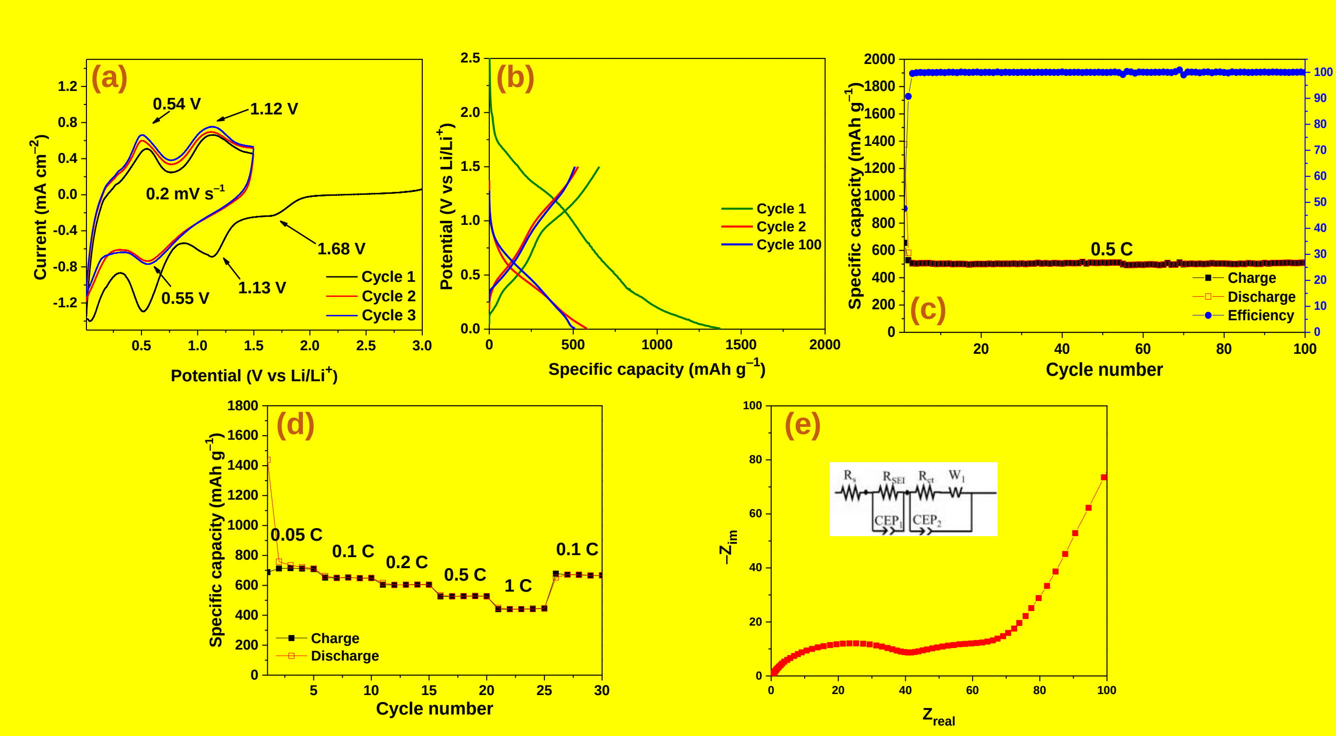

Figure S10. Electrochemical properties of glassy GSSe anodes cycled between 0.01 and 1.5 V vs Li/Li^+: (a) cyclic voltammetry at 0.2 mV s^{-1}; (b) charge-discharge profiles; (c) cycle performance at 0.5 C-rate; (d) rate capability; (e) electrochemical impedance spectroscopy data.

Figure S11.

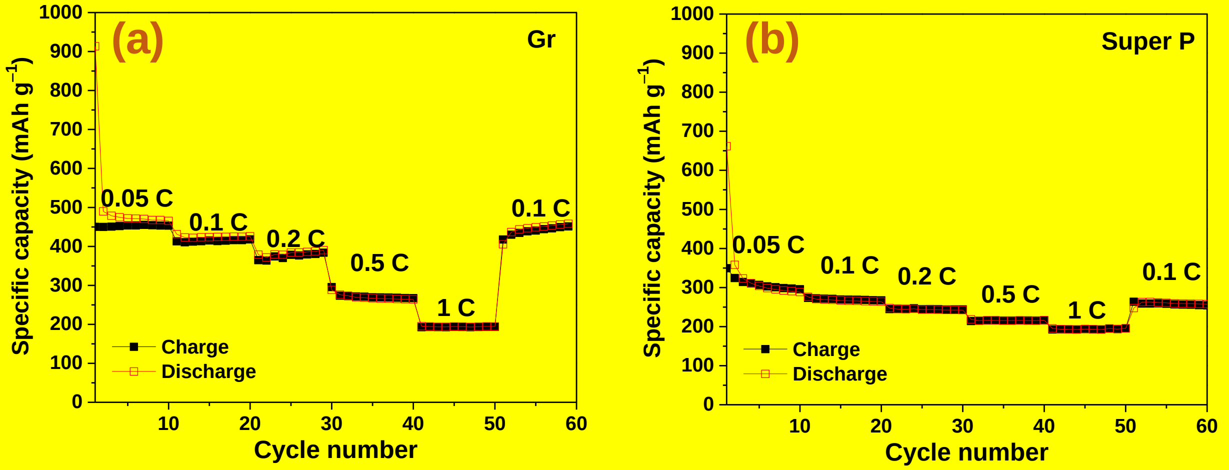

Figure S11. Rate capability studies of graphene and Super P additives.

Figure S12.

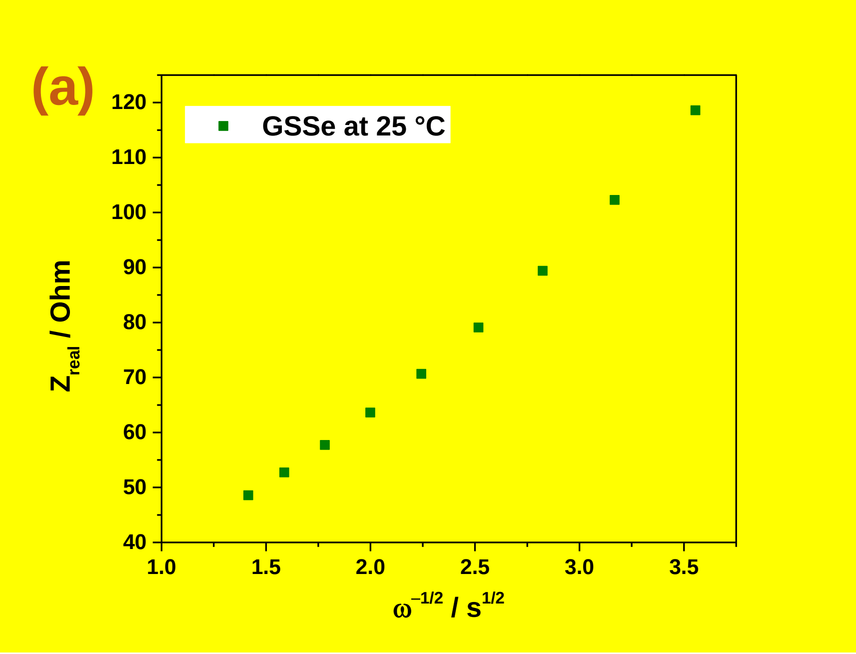

Figure S12. Liner behavior of Z_{real} vs $\omega^{-1/2}$ used calculate the Walburg factor.